Journal Pre-proofs

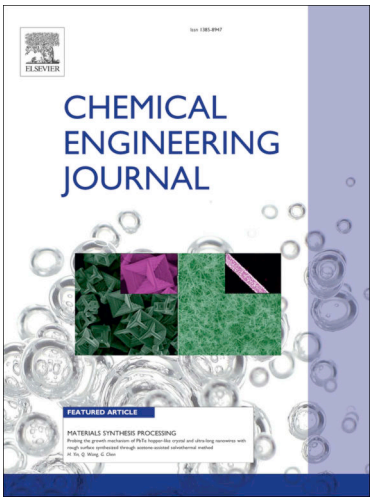

Unlocking the potential of *in situ* H_2O_2 generation in urine as a decentralized electro-sanitation strategy

Raul José Alves Felisardo, Carlos Henrique Magalhães Fernandes, Géssica de Oliveira Santiago Santos, Marcos Roberto de Vasconcelos Lanza

PII: S1385-8947(25)01196-9
DOI: https://doi.org/10.1016/j.cej.2025.160391
Reference: CEJ 160391

To appear in: *Chemical Engineering Journal*

Please cite this article as: R.J. Alves Felisardo, C.H. Magalhães Fernandes, G.d.O. Santiago Santos, M.R. de Vasconcelos Lanza, Unlocking the potential of *in situ* H_2O_2 generation in urine as a decentralized electro-sanitation strategy, *Chemical Engineering Journal* (2025), doi: https://doi.org/10.1016/j.cej.2025.160391

Unlocking the potential of *in situ* H_2O_2 generation in urine as a decentralized electro-sanitation strategy

Authorship and affiliations:

Raul José Alves Felisardo[a,*], Carlos Henrique Magalhães Fernandes[a], Géssica de Oliveira Santiago Santos[a], Marcos Roberto de Vasconcelos Lanza[a,*]

[a]*São Carlos Institute of Chemistry, University of São Paulo, 400 São Carlos, SP 13566-590, Brazil.*

Raul José Alves Felisardo: rfelisardo@usp.br

Carlos Henrique Magalhães Fernandes: chmfernandes@usp.br

Géssica de Oliveira Santiago Santos: gessicasantiago@usp.br

Marcos Roberto de Vasconcelos Lanza: marcoslanza@usp.br

***Corresponding authors:**

E-mail addresses:

Raul José Alves Felisardo: rfelisardo@usp.br

Marcos Roberto de Vasconcelos Lanza: marcoslanza@usp.br

Abstract

This study evaluated the impact of the direct *in situ* generation of hydrogen peroxide (H_2O_2) in urine through the application of gas diffusion electrode based on Printex L6 carbon. The oxidative potential of H_2O_2 was explored to promote the degradation of urea, creatinine, and uric acid. Different current densities (25, 50, 75, and 100 $mAcm^{-2}$) were tested for H_2O_2 electro-generation in Na_2SO_4 under ionic strength and pH conditions similar to those of synthetic urine. The current density of 50 $mAcm^{-2}$ was found to provide the best balance of H_2O_2 production, energy efficiency, and energy consumption; under these conditions, the concentration of H_2O_2 electrogenerated was compared with that accumulated in the urine matrix itself, both in the presence and absence of organic compounds. The results showed that the compositional complexity of urine extends beyond organic compounds, and the significant difference in H_2O_2 generation between Na_2SO_4 and the synthetic inorganic urine matrix can be attributed to the presence of dissociated ions or species generated during the electrolytic process, with active chlorine species playing a notable role. The direct electrogeneration of H_2O_2 in urine resulted in the removal of 43.4% urea, 77.2% creatinine, and 100% uric acid, with partial mineralization of 31% and a lower energy consumption of 6.21 kWh $(g\ TOC)^{-1}$ compared with the process that did not involve the *in situ* generation of H_2O_2. The study highlights a promising strategy for sustainable electro-sanitation practices, offering valuable contributions toward advancing the achievement of the United Nations' Sustainable Development Goals (SDG), particularly in regions with limited access to basic sanitation. By utilizing the urine matrix for in situ hydrogen peroxide generation, this approach fosters decentralized solutions for wastewater treatment.

Keywords: Gas diffusion electrodes, *in situ* H_2O_2 generation, synthetic urine, electro-sanitation, sustainability.

1. Introduction

The Sustainable Development Goals (SDGs), launched in 2015 by the United Nations (UN), represent a global commitment to addressing the most pressing social, economic, and environmental challenges of our planet by 2030 [1]. Among these goals, the SDG 6, which aims to ensure universal access to clean water and adequate sanitation, stands out as one of the most crucial and ambitious goals that are geared toward promoting and safeguarding global public health and well-being. Despite the initial optimism, current projections suggest that we are unlikely to achieve the SDG 6 by 2030, with some estimates extending the timeline for meeting the guidelines and accomplishing the target to 2050 [2]. This concern regarding the inability to accomplish the SDG 6 by the set deadline was reinforced by the 2023 UN World Water Report, which showed that approximately 46% of the global population still lacks access to basic sanitation, while 26% lives without access to safe drinking water [3].

In this context, for the pursuit and accomplishment of the SDGs, scientific research is found to play a key transformative role which involves both collective and individual efforts [4]; specifically, scientific research plays a crucial role when it comes to treating the increasingly complex nature of urban wastewater, including highly challenging effluents such as urine. The complex nature of urine can be primarily linked to its compositional variability, which depends on factors such as age, gender, geographic location, environmental conditions, and diet [5]. Urine primarily contains inorganic compounds such as chloride, sulfate, and phosphate, as well as a high organic load which is derived from its urea, creatinine, and uric acid contents [6,7]. The complex nature of urine makes it difficult to be treated effectively, and this underscores the need for the development of highly efficient technologies that are capable of treating such matrices in an adequate fashion. Centralized wastewater treatment systems have proven to be ineffective when applied for the treatment of urine due to the logistics involved in transporting large volumes of urine [8,9]. For example, an adult produces an average of 1.4 liters of urine per day [5], and this volume is further diluted by water during flushing, where roughly 10 times more water is used for its disposal [10].

This reality points to the urgent need for devising innovative, efficient, and decentralized sanitation solutions for wastewater treatment, especially in remote areas with limited infrastructure [11,12]. Among these approaches, a comprehensive state-of-the-art study published in 2021 highlighted recent efforts to develop urine treatment technologies. This study revealed that while biological processes are effective for urine stabilization, they are not suitable for toilet applications [13]. This limitation can be overcome by advanced oxidation processes (AOP), such as electrochemical oxidation (EO), which has gained prominence among researchers due to the efficiency and flexibility of these processes when applied for the removal of organic compounds from complex matrices [14–16]. The efficiency of EO depends, among other factors, on the electrogeneration of strong oxidants, including hydroxyl radicals, active chlorine species, and hydrogen peroxide (H_2O_2) [17]. H_2O_2 is a versatile oxidant which is widely employed in environmental applications; the *in situ* generation of H_2O_2 offers significant advantages, as it helps eliminate the need for transporting and storing large volumes of reagents [18,19]. H_2O_2 can be generated and accumulated in desirable concentrations during continuous electrolysis, primarily through the two-electron oxygen reduction reaction (ORR), as shown in Eq. 1 [19,20].

$O_2 + 2\ H^+ + 2\ e^- \rightarrow H_2O_2$ (Eq. 1)

The synthesis of H_2O_2 is not an easy task [21], but the underlying difficulties encountered in H_2O_2 generation can be overcome through the use of gas diffusion electrodes (GDE). The use of GDEs allows one to perform electrolysis under ambient pressure and temperature while ensuring that the oxidant is in direct contact with the pollutants in the solution being treated (Carneiro et al., 2016). The efficiency of GDEs for ORR depends, among other factors, on the catalytic material used. Carbon-based materials, such as Printex L6, have demonstrated high efficacy when applied in the construction of catalytic materials; these carbon-based materials have been found to facilitate the occurrence of ORR selectively due to their large surface area and the presence of functional groups in them which help enhance their catalytic activity [23].

Given these well-established advantages of EO, it is clear that the process meets many of the standard prerequisites for application in decentralized wastewater treatment systems. Remarkably, despite the recent progress, significant gaps remain when it comes to devising suitable technologies for the treatment of real and complex matrices such as synthetic urine. Thus, this study aims to investigate the application of electrochemical oxidation with *in situ* H_2O_2 generation and Printex L6 carbon-based gas diffusion electrode (GDE/PL6C) for the efficient treatment of synthetic urine. The primary focus of the study lies in using the proposed treatment mechanism for the degradation of key organic compounds, such as urea, creatinine, and uric acid, whose degradation poses significant challenges to sanitary effluent treatment systems. This study deepens our understanding of advanced treatment processes for complex matrices, providing crucial insights into the development of efficient and affordable technologies for decentralized electro-sanitation practices. In this sense, the present study directly contributes to the development of wastewater treatment solutions which can help accelerate the progress toward the accomplishment of safe and sustainable sanitation goals, including, in particular, the SDG 6.

2. Experimental

2.1. Chemicals and synthetic urine formulation

The synthetic urine matrix was formulated based on a composition described in the literature, as shown in Table 1. All the reagents – acquired from Sigma-Aldrich, used in the experiments were of analytical grade. The solutions were prepared using ultrapure water obtained from a Merck Milli-Q system, with resistivity of 18.2 MΩ cm.

Table 1: Composition of the synthetic urine matrix adapted from Arve and Popat (2021) and Felisardo et al. (2024b) as representative of domestic urine.

Species	Concentration ($molL^{-1}$)

Chemical name	Chemical formula	MW (gmol^{-1})	
Urea	CH_4N_2O	60.06	0.0550
Creatinine	$C_4H_7N_3O$	113.12	0.0015
Uric acid	$C_5H_4N_4O_3$	168.11	0.0003
Sodium chloride	NaCl	58.44	0.1200
Sodium sulfate	Na_2SO_4	142.00	0.0200
Potassium chloride	KCl	74.55	0.0600
Monosodium phosphate	NaH_2PO_4	119.98	0.0200
Total organic carbon (TOC)			750 mg L^{-1}
pH			5.26
Ionic strength			0.3 mol L^{-1}
Conductivity			18.29 mS cm^{-2}

The ionic strength of the solutions was calculated using the Lewis and Randall equation, as expressed in Eq. 2 below [25].

$$\boldsymbol{I = \frac{1}{2}\Sigma C_i Z_i^2} \quad \text{(Eq. 2)}$$

Where I is the ionic strength in mol L^{-1}, C_i is the concentration of ion i in mol L^{-1}, and Z_i is the charge of ion i present in the solution.

2.2. Preparation of GDE with Printex L6 carbon and H_2O_2 electrogeneration

The gas diffusion electrode was prepared based on the standard method developed by our research group [23,26]. Specifically, a catalytic mass of 1.6 g of PL6C, previously dried in an oven for 24 h at 120°C, was mixed with 25 mL of ultrapure water until a completely homogeneous mixture was obtained. Poly(tetrafluoroethylene) (PTFE) (Daflon Co.) was then added to the mixture in a proportion of 20% of the total mass. The mixture was stirred for 45 min at 500 rpm. After that, the resulting catalytic mass was evenly dispersed on carbon cloth attached to a metal mold, and then kept in an oven for 15 min at 120°C in order to obtain a dispersed mass with a moist appearance. Subsequently, the cloth with the PL6C mass was removed from the metal mold, and a second cloth of the same dimensions was placed on top of it. The material prepared was then pressed (SOLAB SL-11) at 0.5 tons, at the temperature of 290°C for 45 min.

Figure 1 presents the operational system used for the conduct of the experiments. The system consisted of a single-compartment cylindrical glass electrochemical cell, equipped with Ag/AgCl reference electrode - from ANALYSER 3A11, a dimensionally stable anode (DSA®) of Ti/RuO_2-TiO_2 used as the counter electrode, and the GDE/PL6C used as the working electrode. The GDE/PL6C and DSA® had a geometric area of 20 cm^2 each. The GDE/PL6C was positioned at the base of the electrochemical cell, where O_2 was injected directly at a fixed flow rate of 0.05 $Lmin^{-1}$. The oxygen flow rate was chosen based on previous studies of our research groups, which indicated that above this value no further improvement in H_2O_2 production is achieved [27]. The temperature of the electrochemical cell was maintained constant at 20°C with the aid of a thermostatic bath (NOVA ÉTICA 521/2D). The system was subjected to mechanical stirring (using FISATOM 710) at 500 rpm. The working volume applied was 250 mL.

For the analysis of H_2O_2 electro-generation, the study initially investigated the role of different current densities (25, 50, 75, and 100 mA cm^{-2}), applied from a MetrohmAutolab PGSTAT-302N Potentiostat, over a period of 120 min in Na_2SO_4, where the same ionic strength and pH of synthetic urine were employed. Subsequently, the concentration of H_2O_2 accumulated in Na_2SO_4 was compared with that generated *in situ* within the synthetic urine matrix, both in the presence and absence of organic compounds, but under the same pH and ionic strength conditions. All the experiments were performed in duplicate, and the average measurements obtained were presented in the study.

2.3 Electrochemical oxidation of the main organic compounds in the synthetic urine matrix

Under specific current density conditions, the electrochemical oxidation (EO) process was applied for the treatment of synthetic urine with and without the *in situ* generation of H_2O_2 in the synthetic urine matrix; the two treatment mechanisms were referred to as EO+H_2O_2 and EO, respectively. The study also analyzed the parallel degradation of the

following organic compounds in the synthetic urine matrix: urea, creatinine, and uric acid. For the EO process, N_2, employed at the same flow rate applied for O_2, was used to prevent H_2O_2 formation.

2.4. Analytical techniques and efficiency analysis

H_2O_2 was quantified using UV-Vis absorption spectrophotometry (SHIMADZU UV-1900), where ammonium molybdate was used as the reagent [28]. The energy consumption (*EC*) associated with the quantification of H_2O_2 was determined using Eq. 3. The current efficiency (*CE*) was estimated based on Faraday's law, as shown in Eq. 4.

$$EC\left(kWh\,Kg^{-1}\right) = 1000\frac{E\,I\,t}{V_s C_{H_2O_2}} \quad \text{(Eq. 3)}$$

$$CE_{H_2O_2}(\%) = \frac{2\,F\,C_{H_2O_2}V_s}{I\,t} \quad \text{(Eq. 4)}$$

Where *E* is the average cell potential (*V*), *I* is the applied current (*A*), *t* is the time (*h*), V_s is the working volume (*L*), and $C_{H_2O_2}$ is the concentration of H_2O_2 generated (mgL^{-1}), 2 is the number of electrons involved in the reduction of one molecule of oxygen to produce H_2O_2, and *F* represents Faraday's constant (96,487 $Cmol^{-1}$).

The degradation of uric acid and creatinine was monitored by high-performance liquid chromatography (HPLC-UVC) using a Shimadzu 20A HPLC system. The analytical column had a C18 stationary phase with a particle size of 5 µm and dimensions of 4.6 mm × 150 mm, and was kept at a constant temperature of 30°C. The experiments were conducted using a fixed injection volume of 20 µL (of the sample). For the analysis of uric acid concentration, a mobile phase consisting of 75:25 (v/v) phosphoric acid (0.1%) and methanol was eluted at a flow rate of 1.0 $mLmin^{-1}$, with UV absorbance (λ) measured at 274 nm. For the analysis of creatinine concentration, a mobile phase of methanol/water in the ratio of 65:35 (v/v) was employed at a flow rate of 0.5 $mLmin^{-1}$, with UV absorbance (λ) measured at 234 nm. All the samples were filtered using Chromafil® Xtra PET-45/25 filters with a pore size of 0.45 µm. Urea concentration was determined using a colorimetric method described in the literature [29]. In this method, solutions containing urea developed a yellow-green color upon reacting with the indicator reagent, p-dimethylaminobenzaldehyde. Absorbance measurements were performed using a spectrophotometer at the wavelength of 420 nm.

The degradation percentage obtained for all the quantified compounds was calculated using Eq. 5, where c_0 represents the initial concentration, and c_t is the concentration at a given electrolysis time.

$$\text{Degradation}\,(\%) = \frac{C_0 - C_t}{C_0}\,100 \quad \text{(Eq. 5)}$$

The amount of energy consumed (*EC*) per unit volume of the treated effluent was determined using Eq. 6, where E_{cell} is the average cell potential (V), t is the electrolysis time (h), V_s is the solution volume (m^3), and I is the current (A).

$$EC\ (Wh\ m^{-3}) = \frac{E_{cell}\ I\ t}{V_s} \quad \text{(Eq. 6)}$$

Total organic carbon (TOC) was analyzed using a Shimadzu TOC-L Series carbon analyzer. The mineralization of the urine solutions was analyzed by monitoring the percentage reduction in TOC, which was calculated using Eq. 7, where TOC_0 represents the initial measurement, and TOC is the value at electrolysis time t. Energy consumption was also evaluated per unit mass of TOC (EC_{TOC}) and calculated using Eq. 8, where, in addition to the description of the parameters described in Eq. 6, $\Delta(\mathrm{TOC})$ represents the content of reduced TOC.

$$\text{TOC removal } (\%) = \frac{\mathrm{TOC_0} - \mathrm{TOC}}{\mathrm{TOC_0}}\ 100 \quad \text{(Eq. 7)}$$

$$\mathrm{EC_{TOC}}\ (\text{kWh (g TOC)}^{-1}) = \frac{E_{cell}\ I\ t}{V_s\ \Delta(\mathrm{TOC})} \quad \text{(Eq. 8)}$$

The kinetic analysis conducted using the plots of c_0/c_t as a function of time consistently pointed to a pseudo-first-order reaction, in line with Eq. 9. In this equation, c_0 denotes the initial concentration, c_t is the concentration at time t, and k_1 is the rate constant for each organic compound.

$$ln\left(\frac{C_0}{C_t}\right) = k_t\ x\ t \quad \text{(Eq. 9)}$$

Carboxylic acids and most of the inorganic ions were identified using ion exchange chromatography with Metrohm Professional IC 850 chromatograph coupled to a Professional IC 940 module. The analysis was conducted using an injection volume of 20 µL of each sample. Carboxylic acids were measured using a MetrosepA Supp 5 column, with 0.5 mmol L^{-1} H_2SO_4 as the eluent. The retention times identified in the chromatograms exhibited well-defined peaks that corresponded to oxalic acid, maleic acid, formic acid, and acetic acid. Nitrogen anions, including nitrite (NO_2^-) and nitrate (NO_3^-), as well as active chlorine species, specifically chloride (Cl^-), chlorite (ClO_2^-) and chlorate (ClO_3^-), were analyzed using a MetrosepA Supp 5 column (150 mm × 4.0 mm) with 3.2 mmol L^{-1} Na_2CO_3 and 1.0 mmol L^{-1} $NaHCO_3$ employed as the eluent, at a flow rate of 0.7 mL min^{-1} and at the temperature of 25°C.

Ammonium cation (NH_4^+) and hypochlorite anion (ClO^-) were identified by UV-Vis spectroscopy. NH_4^+ was identified by the addition of 1 mol L^{-1} NaOH, 5% $C_7H_6O_3$, 5% $Na_3C_6H_5O_7$, 0.05 molL^{-1} NaClO, and 1% sodium nitroferricyanide which led to the formation of a green complex; absorbance was measured at 655 nm [30]. ClO^- was identified when the solutions were in contact with 3 mol L^{-1} NaOH; absorbance was measured at 293 nm. The pH of the solutions was measured using Ion pHB500 pH meter, while conductivity was measured using a Digimed DM-3 conductivity meter.

3. Results and discussion

3.1. Analyzing the effects of current density on *in situ* H_2O_2 electro-generation in Na_2SO_4 using GDE/PL6C

A number of studies conducted to specifically investigate the effects of current density have shown that this parameter is a determining factor in electrochemical processes, as it significantly affects the generation of oxidants such as H_2O_2 [23,26]. A thorough analysis of this parameter is essential for optimizing these processes, as this helps enhance the efficiency and the economic feasibility of wastewater treatment systems. To better understand the effects of current density on the efficiency of the treatment system, GDE/PL6C was used for H_2O_2 electro-generation initially in Na_2SO_4 under ionic strength and pH conditions similar to those of synthetic urine (specifically 0.3 mol L^{-1} and pH = 5.26, respectively). Electrolysis tests were performed at current densities of 25, 50, 75, and 100 mA cm^{-2} in order to evaluate the performance and efficiency of the electrodes (Figure 2a). The results obtained from the monitoring of H_2O_2 concentration over time at different current densities showed a clear pattern: H_2O_2 production increases as current density increases. The doubling of the current density from 25 to 50 mAcm^{-2} resulted in an almost 2-fold increase in the concentration of H_2O_2 accumulated in the system. A similar pattern of behavior was also observed when the current densities of 75 mA cm^{-2} and 100 mA cm^{-2} were applied; these current densities promoted an increase in H_2O_2 production of roughly 3 and 4-fold, respectively, in the system. These results show that the concentration of H_2O_2 produced in the system was directly proportional to the applied current density; this outcome can be attributed to an increase in the electron transfer rate at the electrode/solution interface, which favors the $2e^-$ reduction of molecular oxygen to H_2O_2 at the cathode (see Eq. 1) [31].

Figure 2b supports the aforementioned behavioral pattern observed in the system; the figure shows that the kinetic constant for H_2O_2 production (k), calculated during the first 30 min of electrolysis, increases when the applied current density is increased. However, the linear relationship between these two parameters is not directly proportional across the entire time range and for all current densities. For instance, a 4-fold increase in the current density (from 25 to 100 mA cm^{-2}) resulted in a 7-fold increase in k (from 4.3345 mg L^{-1} min^{-1} to 28.6950 mg L^{-1} min^{-1}); this outcome suggests that although the experimental data fits well with pseudo-first-order kinetics, with R^2 values between 0.97 and 0.99, there is a slight deviation from ideal kinetics, particularly at higher current densities. This deviation could be related to operational factors, such as limited diffusion. At higher current densities, the reaction rate may exceed the rate of O_2 diffusion to the electrode surface, leading to mass

transfer limitations and creating a concentration gradient that hinders H_2O_2 generation during the first 30 min of electrolysis [32,33].

Given the observed deviation in H_2O_2 production kinetics at higher current densities, it is essential to evaluate the effects of current density on energy consumption and current efficiency in order to gain a more comprehensive understanding of the operational feasibility of the treatment system. The EC and CE associated with the electro-generation of H_2O_2 were calculated under the current densities investigated, and the results obtained are presented in Figure 2c. It can be seen that, as the current density increases, there is a significant rise in energy consumption, from 65.99 kWh kg^{-1} at 25 mA cm^{-2} to 193.27 kWh kg^{-1} at 100 mA cm^{-2}. This increase in energy consumption is expected, since the application of higher current densities leads to more power being applied to the system, and this essentially raises the total energy consumed per unit mass of H_2O_2 produced [26].

On the other hand, the current efficiency shows a slight decline with increasing current density, dropping from 10.17% at 25 mA cm^{-2} to 9.38% at 100 mA cm^{-2}. This reduction in CE observed for higher current densities can be attributed to factors such as the occurrence of undesired parallel reactions, including oxygen evolution (Eq. 10) and/or the direct reduction of O_2 to H_2O via the $4e^-$ pathway (Eq. 11) in acidic media [20]. These factors may contribute to a decrease in the proportion of electrons that effectively contribute to H_2O_2 production, reducing the conversion efficiency. Thus, while increasing the current density results in higher H_2O_2 production, it comes at the cost of greater energy consumption and a slight reduction in current efficiency.

$$2H_2O \rightarrow O_2 + 4H^+ + 4e^- \quad \text{(Eq. 10)}$$

$$O_2 + 4\,H^+ + 4\,e^- \rightarrow 2H_2O \quad \text{(Eq. 11)}$$

These results point to the need to optimize the applied current density so as to secure a balance between efficient H_2O_2 production and energy consumption. Thus, the current density of 50 mA cm^{-2} was selected for the conduct of subsequent studies. The choice of this current density was primarily driven by the central goal of this work, which is the treatment of synthetic urine. Given that urine is a complex matrix, it is essential to adopt a moderate current density that can help overcome the inherent challenges brought about by the matrix complexity while promoting the effective degradation of the compounds present there in [15]. Although the current efficiency recorded for 50 mA cm^{-2} is slightly lower than that of 25 mA cm^{-2}, the application of the chosen current density (50 mA cm^{-2}) can help ensure the accumulation of a significant H_2O_2 concentration in the synthetic urine matrix.

3.2. Understanding the mechanism involving the *in situ* electro-generation and accumulation of H_2O_2 in synthetic urine matrix

The compositional complexity of synthetic urine presents additional challenges for the application of electrochemical treatment processes. In addition to organic compounds, this effluent contains a wide range of ionic species that can influence the efficiency of H_2O_2 generation. To have a clearer understanding of the effects of the matrix, a comparative analysis was conducted in order to compare the concentration of H_2O_2 electrogenerated at 50 mA cm^{-2} in Na_2SO_4 with H_2O_2 concentration generated in the synthetic urine matrix, both in the presence and absence of organic compounds; in this study, we refer to the matrix containing organic compounds as synthetic urine matrix and the one without organic compounds as synthetic inorganic urine matrix. For comparative purposes, the same ionic strength and pH were employed in the matrices investigated.

Figure 3a shows the concentration of H_2O_2 generated in the matrices investigated over 120 min of electrolysis. It is observed that throughout the entire period of electrolysis, the concentration of H_2O_2 produced followed this order: Na_2SO_2 > synthetic urine matrix > synthetic inorganic urine matrix. The results obtained point to a significant influence of the compositional complexity of the urine matrix on the efficiency of the H_2O_2 generation process. The Na_2SO_4 solution, used as a simple reference matrix, yielded approximately 505 mg L^{-1} of H_2O_2 after 120 min of electrolysis. However, when the synthetic urine matrix containing organic compounds - including urea, creatinine, and uric acid, was employed, the concentration of H_2O_2 generated was reduced to 175 mg L^{-1} by the end of the process. This substantial decrease in H_2O_2 production can be attributed to the presence of organic compounds in the urine, which consume H_2O_2 in the degradation process or compete for the same electrons that would be used in the reduction of molecular oxygen to form H_2O_2. This behavior is further supported by the fact that, after 45 min of electrolysis, there is a stabilization in the concentration of H_2O_2 produced in the synthetic urine matrix (which contains organic compounds); this phenomenon can be attributed to the chemical equilibrium established between the H_2O_2 formation reactions at the cathode and the H_2O_2 degradation reactions at the anode [26,34].

When the organic compounds were removed from the synthetic urine matrix; i.e., when the synthetic inorganic urine matrix was employed, there was a further reduction in the concentration of H_2O_2 generated, with H_2O_2 production beginning only after 15 min of electrolysis and reaching a mere 61.3 mg L^{-1} by the end of the process. These results are evidently surprising and go counter to our initial expectation that the concentration of H_2O_2 generated in the synthetic inorganic urine matrix would be greater than that of the synthetic urine matrix (containing organic compounds). This observation suggests that, in addition to the organic compounds, the ionic composition of the urine itself exerts a significant effect on the efficiency of H_2O_2 electrogeneration, as the complex mixture of ions may influence the reactions at the electrode/solution interface. Another explanation for this unexpected outcome is that, in the absence of organic compounds, the active species formed in the inorganic reaction medium (synthetic inorganic urine matrix), such as active chlorine species, are free to act as H_2O_2 scavengers. In other words, without the presence of organic matter to be degraded, these active species, which would typically participate in the degradation of organic compounds, end up more intensely capturing and decomposing the H_2O_2 generated.

Through a careful analysis of the data on energy consumption and current efficiency (Figure 3b), one is able to have a better understanding of the mechanism involving the efficiency of H_2O_2 electro-generation in urine matrices and the effect of their complex nature on the efficiency of the treatment system. The application of the Na_2SO_4 solution as the

reaction medium resulted in the lowest energy consumption (113.45 kWh kg^{-1}) and the highest current efficiency (9.96%). These results point to the effectiveness of the GDE/PL6C and the electrochemical system when applied to a less complex solution, where the H_2O_2 generation reaction occurs more efficiently, with reduced energy loss which stems from secondary reactions or resistive effects. However, the *in situ* electro-generation of H_2O_2 in the synthetic urine matrix, which, in addition to Na_2SO_4, contains NaCl, KCl, NaH_2PO_4, and organic compounds including urea, creatinine, and uric acid, led to more than a 2-fold increase in energy consumption (277.12 kWh kg^{-1}), while current efficiency decreased to 3.27%. These results can be attributed to the presence of organic compounds that consume H_2O_2 during the degradation process or compete for electrons, diverting the action of the current toward parallel reactions. When the synthetic inorganic urine matrix was used as the reaction medium, there was a significant increase in energy consumption (725.92 kWh kg^{-1}), while current efficiency dropped to 1.21%. This outcome helps confirm that the high ionic complexity of the synthetic urine matrix undermines the overall efficiency of the H_2O_2 generation process; in essence, this highlights the need to investigate each compound separately so as to have a better understanding of their effects, thus contributing toward optimizing the electro-sanitation treatment process.

3.3 Unraveling the influence of the compositional complexity of synthetic inorganic urine matrix on the electro-generation of H_2O_2

As pointed out previously, the complexity of the synthetic inorganic urine matrix poses a significant challenge to the electrogeneration of H_2O_2; this challenge arises because the ions present in this matrix, including SO_4^{2-}, Cl^-, and PO_4^{3-}, can interact with H_2O_2, reducing its availability in the medium and/or promoting competitive reactions. With this in mind, and to identify which of these compounds act as true interferents, H_2O_2 generation was analyzed individually for each of the constituent salts in the urine matrices. This analysis was conducted using the same ionic strength and pH of synthetic urine at a current density of 50 mA cm^{-2} over a period of 120 min of electrolysis. Figure 4 presents a comparative analysis of the concentration of H_2O_2 generated in NaCl, KCl, and NaH_2PO_4 compared to that generated in Na_2SO_4 and in the urine matrices investigated.

The results obtained showed significant variations in the concentration of H_2O_2 generated over the electrolysis time in the different electrolytes (of synthetic urine) employed. When Na_2SO_4 was applied, there was a consistent increase in H_2O_2 generation over time. A much lower H_2O_2 production was recorded for KCl, where only 50.8 mg L^{-1} was produced at the end of 120 min of electrolysis. NaCl, in contrast, exhibited intermediate production levels, yielding 70.5mg L^{-1} of H_2O_2 over the same period. Interestingly, NaH_2PO_4 recorded the highest concentration of H_2O_2 produced, reaching stabilization in around 30 min of electrolysis, and accumulating approximately 330 mg L^{-1} of H_2O_2 after 120 min of electrolysis.

The results obtained show that distinct chemical interactions impact the efficiency of the electrochemical process; in general terms, the results suggest that KCl and NaCl act more intensely as inhibitors in the generation of H_2O_2 compared to NaH_2PO_4 and Na_2SO_4. When

one focuses the analysis on the isolated anionic species, the results imply that the higher generation of H_2O_2 in Na_2SO_4 (Figure 4a) can be attributed to the fact that the sulfate anion (SO_4^{2-}) does not significantly interfere with the oxygen reduction process at the electrode surface, and this allows for a more efficient conversion of O_2 to H_2O_2. However, it is important to note that although sulfate is considered an inert anion when it comes to H_2O_2 generation for comparative purposes in this study, the production of peroxomonosulfate (SO_5^{2-}) can also occur during the electrochemical process involving the use of GDE/PL6C, as shown in Eq. 12. SO_5^{2-} is regarded as a predatory species of H_2O_2 which reacts with itself, as indicated in Eq. 13 [23].

$$H_2O + SO_4^{2-} \rightarrow 2H^+ + 2e^- + SO_5^{2-} \quad \text{(Eq. 12)}$$

$$H_2O_2 + SO_5^{2-} \rightarrow 2O_2 + H_2SO_4 \quad \text{(Eq. 13)}$$

Regarding NaH_2PO_4, as demonstrated in Figure 4a, the relatively lower concentration of H_2O_2 generated compared to that produced in Na_2SO_4 can be explained by the reaction between the dihydrogen phosphate ion ($H_2PO_4^-$) and H_2O, which leads to the formation of hydroxyl radicals ($^{\bullet}OH$), as shown in Eq. 14 and Eq. 15 [14,35]. This mechanism suggests that, although a direct reaction between $H_2PO_4^-$ and H_2O_2 is uncommon, the higher $^{\bullet}OH$ concentrations present in the solution may react with the H_2O_2 generated, converting it into H_2O (Eq.16), and thereby reducing the availability of H_2O_2 in the medium. Furthermore, phosphate may form complexes that accelerate the decomposition of H_2O_2 and may also play a dual role in generating reactive oxygen species (ROS) that facilitate the formation of $O_2^{\bullet-}$ and alter the pathway of $^{\bullet}OH$ formation, further decreasing the concentration of H_2O_2 in the treated solution [36]. The stabilization observed in H_2O_2 production after 30 min of electrolysis can be attributed precisely to the phosphate ability to form these complexes, which, in interaction with other anionic species and/or intermediate radical species, can diminish the decomposition of H_2O_2 and stabilize its concentration in the solution.

$$H_2O + HPO_4^{2-} \rightarrow {}^{\bullet}OH + H_2PO_4^- \quad \text{(Eq. 14)}$$

$$H_2PO_4^- + {}^{\bullet}OH \rightarrow H_2PO_4^{\bullet} + OH^- \quad \text{(Eq. 15)}$$

$$^{\bullet}OH + H_2O_2 \rightarrow 2H_2O + O_2 \quad \text{(Eq. 16)}$$

On the other hand, the accumulated concentration of H_2O_2 recorded in KCl and NaCl was significantly lower than that recorded in Na_2SO_4 after 120 min of electrolysis (results are more clearly visible in the scale of Figure 4b). This phenomenon observed in chloride media can be attributed to the influence of active chlorine species formation. It has been well documented in the literature that the oxidation of chloride ion (Cl^-) on the anode surface leads to the generation of chlorine ($Cl_{2(aq)}$, E°= 1.36 V vs SHE), as shown in Eq. 17. Chlorine subsequently undergoes hydrolysis to produce hypochlorous acid (HClO, E°= 1.49 V vs SHE) and $Cl^–$, as per Eq. 18. Under specific speciation conditions (pKa = 7.55), HClO enters an acid-base equilibrium, and this leads to the production of hypochlorite ($OCl^–$, E° = 0.89 V vs SHE), as demonstrated in Eq. 19. After the occurrence of this reaction, the active chlorine species consume H_2O_2 through secondary reactions, as exemplified in Eqs. 20, 21, and 22, respectively, for Cl_2, HOCl, and $OCl^–$ [37–39].

$$2Cl^– \rightarrow Cl_2 + 2e^– \quad \text{(Eq. 17)}$$

$$Cl_2 + H_2O \rightarrow HClO + Cl^– + H^+ \quad \text{(Eq.18)}$$

$$HClO \leftrightarrows OCl^– + H^+ \quad \text{(Eq. 19)}$$

$$H_2O_2 + Cl_2 \rightarrow O_2 + 2H^+ + 2Cl^– \quad \text{(Eq. 20)}$$

$$H_2O_2 + HOCl \rightarrow O_2 + H_2O + H^+ + Cl^– \quad \text{(Eq. 21)}$$

$$H_2O_2 + OCl^– \rightarrow O_2 + H_2O + Cl^– \quad \text{(Eq. 22)}$$

In summary, for the electro-generation and accumulation of H_2O_2 in the synthetic inorganic urine matrix, which is specifically constituted by Na_2SO_4, NaCl, KCl, and NaH_2PO_4, as previously discussed, we found that this matrix yielded a relatively lower concentration of H_2O_2 compared to Na_2SO_4 and the other media studied individually. This behavior shows that an increase in the complexity of the reaction medium contributes to the reduction in the concentration of H_2O_2 generated; this is likely due to increased parasitic reactions involving inorganic ions and/or other causes mentioned previously. These results point to the complexity of the synthetic urine matrix when used in the electro-generation of H_2O_2; in essence, the results suggest that, in order to optimize H_2O_2 production in wastewater treatment systems involving urine, it is essentially crucial to have a thorough understanding of the synergistic and inhibitory effects of the various compounds present in the matrix, and of

other related factors. Thus, having a comprehensive understanding of the processes involving the degradation and mineralization of organic compounds in urine through electrochemical oxidation with and without *in situ* H_2O_2 generation is crucial for devising efficient strategies for the treatment of sanitary wastewater.

3.4. *In situ* generated H_2O_2 in synthetic urine and its effect on the degradation and mineralization of organic matter

Urine is a matrix of complex composition, and the presence of organic compounds, such as urea, creatinine, and uric acid, in it presents additional challenges for electrochemical treatment processes. Understanding the potential of *in situ* generated H_2O_2 in degrading these compounds in the urine matrix is essential for developing effective electro-sanitation treatment strategies. Figure 5a shows the parallel degradation percentages obtained for the organic compounds present in urine during the electrochemical process based on the application of the GDE/PL6C cathode in the presence (EO+H_2O_2) and absence of H_2O_2 generation (EO) at the current density of 50 mA cm^{-2}. It is worth noting that, in the EO process, N_2 was injected into the GDE/PL6C, instead of O_2, equivalent to 0.05 $Lmin^{-1}$. The results obtained pointed to significant differences between the EO+H_2O_2 and EO processes, in terms of the degradation and mineralization of organic compounds in urine; importantly, the results show that H_2O_2 was effectively beneficial for the degradation of urea and creatinine.

Urea (CH_4N_2O) is the predominant organic compound in human urine; its structure is quite dynamic, and the compound can exhibit various conformational variations when in aqueous solution [40]. As illustrated in Figure 5a, urea is the organic compound that was found to be the most resistant to degradation in the EO+H_2O_2 and EO processes; the application of the EO+H_2O_2 and EO processes led to urea degradation of 43.4% and 35.1%, respectively, after 120 min of electrolysis. The lower removal of urea compared to other compounds may be attributed to competitive degradation among the co-existing compounds. Furthermore, considering that urea is present in much higher concentration in the medium, approximately 20 times more than creatinine and 65 times more than uric acid, it is likely that greater rates of urea removal would require longer treatment times. The percentage difference in urea degradation observed between the EO+H_2O_2 and EO processes was 8.3%. Although this percentage is relatively low, it represents approximately 273.0 mg L^{-1} in absolute terms; this shows that the presence of in situ generated H_2O_2 in urine has a positive effect on urea degradation. These observed improvements in the compounds degradation efficiency provide us with useful insights into the development of more effective strategies for the treatment of sanitary effluents, where urea is one of the primary pollutants to be degraded.

Another relevant point that deserves mentioning is that H_2O_2 can also be explored as an inhibitor of the process involving the hydrolysis of urea in real urine systems [41]. This is particularly relevant given the inherent instability of urea, which rapidly decomposes in the presence of urease, an enzyme commonly found in urine collection systems. During this process, urea breaks down into ammonium ions and bicarbonate, as described in Eq. 23 [42,43]; this enzyme is naturally present in both urine and the environment [8]. After the hydrolysis process, the pH of the medium increases to a value above 9.0 [44]. The inactivation

of urease by H_2O_2 in real urine systems - which blocks the hydrolysis of urea, prevents the increase in soil pH and consequently reduces the risk of eutrophication in water bodies, as well as the release of free ammonia into the atmosphere [45].

$$CH_4N_2O + 2H_2O \rightarrow NH_3 + NH_4^+ + HCO_3^- \quad \text{(Eq. 23)}$$

Regarding creatinine ($C_4H_7N_3O$) - the second most abundant compound in the urine matrix, Figure 5a shows that both treatment processes tested in the study were effective in degrading it, with 77.2% and 68.6% creatinine degradation recorded for EO+H_2O_2 and EO processes, respectively. We noted that the treatment process that involved H_2O_2 electro-generation (EO+H_2O_2) was 8.6% more efficient; in other words, this process was able to remove an additional 14.3 mg L^{-1} of creatinine compared to the process without H_2O_2 generation. Although the observed difference is relatively smaller in comparison with urea degradation, it still shows that the presence of *in situ* generated H_2O_2 enhances the oxidation process. The higher rate of degradation of creatinine relative to urea may be attributed to the following: lower concentration of creatinine in the matrix, and competitive oxidation with other compounds present in the synthetic urine matrix [15].

On the other hand, the degradation of uric acid ($C_5H_5N_4O_3$) - the smallest organic compound in the synthetic urine matrix, was satisfactorily efficient in both the EO+H_2O_2 and EO processes, since both processes recorded 100% uric acid removal, as shown in Figure 5a. These findings show that the electrochemical oxidation process alone is sufficient for the degradation of uric acid in the synthetic urine matrix, and that H_2O_2 may not be necessary for the complete degradation of the compound. However, H_2O_2 can play a complementary role, particularly in scenarios where the matrix is more complex or where other compounds may interfere with the process efficiency, especially in the degradation of by-products or intermediate compounds generated during the oxidation of uric acid. These results are consistent with previous studies reported in the literature which have demonstrated the efficiency of the electrochemical oxidation process when applied for the degradation of uric acid in urine [15,46–48]. The system preference for the degradation of uric acid over urea and creatinine may be due to the presence of multiple functional groups in the structure of uric acid [46].

In some literature studies, in addition to EO and EO+H_2O_2, other advanced processes have been explored for the treatment of synthetic urine, particularly for the removal of pharmaceuticals in this effluent. Goulart et al. demonstrated that photolysis and photoelectrolysis were effective in the degradation of the antibiotic levofloxacin in synthetic urine, while showing that creatinine and uric acid were degraded together with the antibiotic during the processes [46]. Similarly, Gonzaga et al. reported that the Electro-Fenton (EF) and Photoelectro-Fenton (PhEF) processes are also viable technologies for the treatment of synthetic urine contaminated with Penicillin G. In their study, the authors showed that the PhEF process was more efficient than EF in the degradation of the pharmaceutical, with the best results achieving complete degradation in synthetic urine [49].

The analysis of the operational costs of the treatment system, particularly energy demand, is crucial when it comes to assessing the efficiency of the technologies employed for wastewater treatment and the degradation of unwanted organic pollutants [50]. The energy consumed per volume of the treated effluent in the EO and EO+H_2O_2 processes was estimated using Eq. 5; the results obtained are presented in Figure 5b. As can be observed, the results show that in order to remove 43.4% of urea, 77.2% of creatinine, and 100% of uric acid, the EO+H_2O_2 process consumed 46.32 kWh dm^{-3} of energy; in contrast, the EO process required 56.18 kWh dm^{-3} to remove the same percentage of uric acid and relatively lower percentages of urea and creatinine compared to the EO+H_2O_2 process. This increase in energy consumption of nearly 10 kWh dm^{-3} in the EO process further underscores the importance of H_2O_2 in enhancing the overall efficiency of the electrochemical process; in essence, this outcome reinforces the role of H_2O_2 as a critical element when it comes to developing efficient wastewater treatment technologies.

Another fundamental analysis when it comes to evaluating the overall efficiency of electrochemical treatment techniques is the mineralization process. In complex matrices, such as the synthetic urine used in this study, having a clear understanding of the mineralization process is essential to ensuring the complete conversion of organic matter to CO_2, H_2O, and inorganic ions. Figure 5c shows the kinetic curve and the TOC removal rates recorded for the EO and EO+H_2O_2 processes during 120 min of electrolysis at the current density of 50 mA cm^{-2}. Regarding the kinetics of mineralization, the two processes exhibited a similar behavior, with no significant differences in TOC reduction up to approximately 30 min of electrolysis. After this period, the EO+H_2O_2 process once again demonstrated higher efficiency compared to the EO process. At the end of the electrolysis, the partial mineralization achieved was 31.8% and 22.5% for EO+H_2O_2 and EO, respectively. In absolute terms, considering the presence of high TOC in the urine matrix (TOC_i = 750 mg L^{-1}), the difference in the TOC removal percentage between the processes, as indicated in Figure 5d, corresponds to 68.6 mg L^{-1}; this value is found to be highly significant for the mineralization process and shows that H_2O_2 also plays an influential role in mineralization. The difference between the two treatment processes is also evident in the estimated energy consumption per unit mass of TOC removed, calculated using Eq. 7 and presented in Figure 5d. Notably, the EO+H_2O_2 process exhibited a lower energy consumption of 91.9 kWh kWh (g TOC)$^{-1}$compared to 98.1 kWh (g TOC)$^{-1}$ for EO alone. This reduction highlights the positive contribution of in situ H_2O_2 generation in enhancing the process efficiency. Although the absolute values remain high, the observed decrease suggests that H_2O_2 plays a role in facilitating organic compound degradation, ultimately leading to a more energy-efficient approach within the studied system.

Despite the difference in TOC removal rates observed between the EO+H_2O_2 and EO processes, the unimpressive mineralization rate of 31.8% recorded for the EO+H_2O_2 process can primarily be attributed to the partial degradation of urea, considering that this compound accounts for about 90% of the TOC in the matrix. Similarly, the tendency for stabilization in TOC removal observed after 45 min of electrolysis in both the EO+H_2O_2 and EO processes (see Figure 5c) point to the formation of recalcitrant species which are resistant to the mineralization process. These findings are also consistent with previous studies [15,48,51] and point to the need for further investigation and the development of highly efficient processes for the treatment of complex and real matrices.

The findings highlight the importance of considering the concentration and dynamics of organic compounds in complex matrices to optimize electrochemical processes. This need

is particularly emphasized in real systems, where the inclusion of H_2O_2 generated in situ, based on the matrix's composition, serves as an effective strategy for enhancing the removal of resistant compounds. Such an approach is especially crucial for the treatment of sanitary effluents, as *in situ* generation of H_2O_2 enables decentralized treatment actions. In the case of urine, this strategy is highly recommended due to the logistical challenges of transporting large volumes of effluent to centralized systems. Consequently, these strategies not only improve the efficiency of treatment but also offer a more sustainable approach for managing wastewater, including its discharge to urban wastewater treatment plants.

3.5 Kinetic analysis of the degradation of organic compounds in synthetic urine based on the application of EO+H_2O_2 and the role of active chlorine species

The kinetic analysis of organic compounds degradation in the synthetic urine matrix under the EO+H_2O_2 process is essentially crucial because it helps boost our understanding of the dynamics involving the removal of different compounds (urea, creatinine, and uric acid) which co-exist in complex systems. The organic compounds in complex matrices exhibit different reactivities toward oxidative processes, and this leads us to obtain different rates of degradation of the compounds (see Figure 5a) which occur simultaneously in the treatment system. Understanding the behavior of these co-existing compounds in the urine matrix over the course of the treatment process is essential for developing effective strategies for the treatment of sanitary effluents and for boosting their application in real systems.

Figure 6a shows the gradual decline in the normalized concentration of urea, creatinine, and uric acid under the EO+H_2O_2 process, applied at the current density of 50 mA cm^{-2} in 120 min of electrolysis. The temporal analysis indicated that the first 60 min of electrolysis were more efficient for the degradation of urea and creatinine, with approximately 31% and 68% removal rates recorded for the compounds, respectively. In contrast, uric acid was more susceptible to oxidation; this compound was completely removed within the first 10 min of electrolysis. The observed decrease in the process efficiency with increased electrolysis time, particularly after the initial 60 min, where an additional removal of only about 11% of urea and 8% of creatinine was recorded in the subsequent hour, may be attributed to the reduced concentration of these compounds that remained in the system. This reduction in the concentration of the compounds (urea and creatinine, in this case) leads to diminished substrate availability for oxidation reactions. As the concentrations of urea and creatinine decrease over time, competition for oxidizing species, such as H_2O_2, becomes less intense. These observations suggest that the kinetics of organic compounds degradation in urine reflect not only the individual properties of each substance but also the complex interactions occurring within the medium.

In real systems, where multiple organic compounds are present, the concurrent degradation of these compounds can significantly impact the efficiency of the process. This competition dynamics involving the compounds can be analyzed through a comparison of their respective rate constants [52]. Figure 6b presents the corresponding pseudo-first-order kinetic rate constants obtained for the concentration decay shown in Figure 6a. Looking at the

strong correlations observed up to 30 min of electrolysis, the rate constants obtained were 0.0057, 0.0344, and 0.5441 min^{-1} for urea, creatinine, and uric acid, respectively.

In our present study, considering the rapid decay of uric acid concentration relative to urea and creatinine, the ratio $k_{uric\ acid}/k_n$ was used to analyze the competitive dynamics involving the organic compounds present in the synthetic urine matrix. In this analysis, k_n represents the kinetic degradation constant of either urea or creatinine. A ratio > 1 indicates a preference for the degradation of uric acid over the other compounds, whereas a ratio < 1 indicates the preference for the degradation of urea or creatinine over uric acid [46]. The analysis of the competitive action among the compounds yielded $k_{uric\ acid}/\ k_{urea}$ ratio = 95.46 and $k_{uric\ acid}/\ k_{creatinine}\ ratio$ = 15. These results, which are consistently > 1, show that the system has a preference for the removal of uric acid over urea and creatinine, with the degradation rate of uric acid being approximately 100 times greater than that of urea and about 15 times faster than that of creatinine. Among the factors that affect the degradation process, the concentrations of the compounds play a crucial role. As previously noted, in the presence of higher initial concentration of the compounds, the system may require more time to achieve certain removal rates. In the case of uric acid, its comparatively lower concentration relative to urea and creatinine is expected to facilitate its faster degradation. In addition, the presence of multiple functional groups in uric acid may have been a determining factor for its higher and faster degradation rates.

It is worth noting that, in addition to direct oxidation and the action of H_2O_2, other species formed during the process can also act as oxidants for the organic matter present in urine. Among these species, hydroxyl radicals (•OH) and chlorinated species are particularly relevant. The diffusion of these electroactive species toward the anode plays a crucial role, as this can influence both the distribution and availability of the compounds to be degraded [15]. Regarding •OH, the dimerization of DSA (•OH) can lead to the formation of H_2O_2, as shown in Eq. 24, and both species can subsequently react to form the hydroperoxyl radical (DSA(HO_2•)), a weak oxidant, as per Eq. 25[15].

$$2DSA(^{\bullet}OH) \rightarrow 2DSA + H_2O_2 \qquad \text{(Eq. 24)}$$

$$DSA(^{\bullet}OH) + H_2O_2 \rightarrow DSA(HO_2^{\bullet}) + H_2O \qquad \text{(Eq. 25)}$$

Regarding chlorinated species, Cl^- can be oxidized to Cl_2 (seeEq.17), which can then undergo deprotonation to form ClO^-, as indicated in Eq. 26. On the other hand, the ClO^- generated can undergo consecutive anodic oxidation to produce ClO_2^-, ClO_3^- and ClO_4^-, as described in Eqs. 27, 28, and 29, respectively[15].

$$Cl_2 + 2OH^- \rightarrow ClO^- + Cl^- + H_2O \qquad \text{(Eq. 26)}$$

$$ClO^- + H_2O \rightarrow ClO_2^- + 2H^+ + 2e^- \quad \text{(Eq. 27)}$$

$$ClO_2^- + H_2O \rightarrow ClO_3^- + 2H^+ + 2e^- \quad \text{(Eq. 28)}$$

$$ClO_3^- + H_2O \rightarrow ClO_4^- + 2H^+ + 2e^- \quad \text{(Eq. 29)}$$

In this context, thorough analyses were conducted in order to monitor the changes in pH and Cl^- ions, as well as the evolution of ClO^-, ClO_2^-, and ClO_3^- species in synthetic urine matrix based on the application of the EO+H_2O_2 process, at the current density of 50 mA cm^{-2}, for a period of 120 min (of electrolysis) (Figure 7). As can be observed, during the first minutes of treatment, the initial pH of the synthetic urine was 5.26, and the matrix exhibited a high concentration of chloride ions and a modest formation of 2.7 mg L^{-1} of ClO_3^- within the first 10 min of electrolysis, with no ClO^- or ClO_2^- species detected. As the electrolysis time progressed and the solution pH increased, there was a decrease in the chloride ions concentration, while the concentrations of both chlorinated species increased. This rise in the generation of chlorinated species points to the progressive conversion of chloride ions into their oxidized forms - a phenomenon also reported in the literature [53,54]. After 45 min of electrolysis, with a pH ranging between 6.39 and 6.60, the concentrations of ClO_2^- and ClO_3^- surpassed that of ClO^- and continued to exhibit a gradual increase until the end of the process. On the other hand, ClO_2^- and ClO_3^- concentrations of 43 and 65 mg L^{-1}, respectively, were recorded at the end of the 120 min of electrolysis. These observations evidently reinforce the presence of competition between the electro-generation of H_2O_2 and the evolution of chlorine species, particularly Cl_2 and ClO^-, as demonstrated in Eqs. 17-22.

Notwithstanding the competition between the electro-generation of H_2O_2 and the evolution of chlorine species, the accumulated concentration of ClO^-, which was approximately 21 mg L^{-1}, is found to be significant considering that hypochlorite/hypochlorous acid acts as the primary mediator in electrochemical processes in the presence of Cl^- [55]. Furthermore, ClO^- can be generated within a pH range of 3.0 to 8.0, and the species is capable of reacting with organic compounds more rapidly than other species due to its reaction homogeneity throughout the solution under treatment. In contrast, oxidation facilitated by DSA (•OH), for instance, is restricted to the anode surface, as this species has a very short lifespan [15]. Thus, during the EO+H_2O_2 process, the organic compounds in synthetic urine are expected to undergo simultaneous oxidization by both H_2O_2 and ClO^-, with lesser contribution from DSA (•OH).

These findings allowed us to conduct a quantitative analysis that provided valuable insights into the degradation of organic compounds in synthetic urine and their individual contributions to the electrochemical process. The observed dynamics reflect the complex interaction between direct and indirect oxidation involving H_2O_2, chlorinated species, and hydroxyl radicals in the organic matter removal process.

3.6. Evolution of carboxylic acids and destination of nitrogen ions in the treatment of synthetic urine under the EO+H_2O_2 process

Given the importance of the mineralization process in synthetic urine matrices, a thorough analysis was conducted in order to identify and quantify the intermediate products derived from the treatment of 3,303.3 mg L^{-1} of urea, 169.7 mg L^{-1} of creatinine, and 50.4 mg L^{-1} of uric acid (TOC_i = 750 mg L^{-1}) based on the application of the EO+H_2O_2 process at the current density of 50 mA cm^{-2}. Figures 8a and 8b show the time course of accumulated short-chain linear aliphatic carboxylic acids; these acids - with special reference to oxalic acid and maleic acid, were found to be significantly accumulated in the system during the treatment.

The initially high concentration of oxalic acid in the system (Figure 8a), approximately 88 mg L^{-1} in 15 min, reflected a stabilization pattern observed throughout the process, with minimal fluctuations recorded up to the end of the 120 min of electrolysis. This behavior suggests that oxalic acid is rapidly formed and remains a stable intermediate, resisting complete mineralization in the synthetic urine matrix. Conversely, maleic acid (Figure 8a), which also began with a high concentration of about 440.0 mg L^{-1} in 15 min, recorded a significant reduction in its concentration, reaching approximately 205.0 mg L^{-1} in 30 min, and subsequently stabilizing at around 230.0 mg L^{-1}. This more pronounced fluctuation and the decrease in concentration compared to that observed in the first 15 min may be indicative of the partial transformation of maleic acid into other by-products or a subsequent deeper oxidation process. In contrast, formic and acetic acids (Figure 8b), which began being accumulated in a more modest fashion, saw a gradual increase in their concentration over the electrolysis time. Formic acid increased from approximately 3.8 mg L^{-1} in 15 min to 14.8 mg L^{-1} in 120 min, while acetic acid increased from 0.96 mg L^{-1} in 30 min to approximately 4.7 mg L^{-1} in 120 min. This progressive accumulation suggests that these acids (formic and acetic acids) are formed at a slower rate.

It is likely that acetic acid is derived from the cleavage of aromatic and conjugated rings [56], while oxalic and formic acids may originate from the oxidation of other long-chain carboxylic acids [57,58]. These results show that, despite the partial degradation of organic compounds in the synthetic urine matrix, the considerable accumulation of carboxylic acids as intermediates explains why a maximum mineralization of only 31.8% was obtained. This is evidenced by the remaining TOC content in the synthetic urine solution at the end of the process - approximately 504.0 mg L^{-1} (see Figure 5c), of which about 24% was composed of carboxylic acids, primarily maleic acid, which corresponded to a TOC of 92.4mg L^{-1}. Interestingly, despite their resistance to mineralization, literature reports indicate that these low molecular weight carboxylic acid species are considered innocuous and biodegradable [51,58].

Regarding inorganic ions, as expected, the main products detected were ammonium (NH_4^+) and nitrate (NO_3^-) due to the presence of urea (N = 1540.52 mg L^{-1}), creatinine (63.03 mg L^{-1}), and uric acid (N = 16.81 mg L^{-1}) in the synthetic urine composition; the presence of these products in the matrix resulted in a high total nitrogen concentration of 1620.4mg L^{-1}. Nitrite (NO_2^-) was not found in significant concentrations. As observed in Figure 8c, one can clearly see an increase in the concentration of NH_4^+ up to approximately 42 mg L^{-1} in 15 min. From this time onwards, there is a decrease in NH_4^+ concentration, accompanied by a gradual

accumulation of NO_3^- which remains as the final product after 120 min of electrolysis (representing 2.77% of the initial N). These results suggest that the gradual conversion of ammonia to nitrate reflects the primary reduction of nitrogen to more oxidized species. Considering the contribution of urea, creatinine, and uric acid to the nitrogen content in the system, it can be inferred that the rapid accumulation of NH_4^+ up to the first 15 min was mainly due to the rapid decomposition of uric acid. Furthermore, considering the initial nitrogen content and the fact that the final accumulated concentration of nitrogen ions did not exceed 46.3 mg L^{-1}, one can infer from a general mass balance that over 97% of the initial nitrogen content remained in the form of the original molecules of urea and creatinine, or was lost from the synthetic urine solution as volatile products such as N_2 and N_xO_y [58].

4. Conclusions

This study investigated the potential of using *in situ* H_2O_2 generation in synthetic urine with GDE/PL6C as a decentralized electro-sanitation strategy. The initial results indicated that the *in situ* electro-generation of H_2O_2 in Na_2SO_4 solution, under the same pH and ionic strength of synthetic urine, directly correlates with the applied current density. The final results obtained showed that the application of a current density of 25 mA cm^{-2} generated 258.0 mg L^{-1} of H_2O_2, which increased to 958.0 mg L^{-1} when the current density was raised to 100 mA cm^{-2}. This outcome was attributed to an increase in the electron transfer rate at the electrode/solution interface. However, kinetic analysis suggested that at higher current densities, H_2O_2 production did not follow a linear pattern; this points to limitations in the mass transfer process. The choice of using the current density of 50 mA cm^{-2} to investigate the performance of the system was justified by the fact that the proposed system required the application of a relatively high current density with economic viability which offers a balance between energy efficiency and energy consumption efficiency with high H_2O_2 production and effective compounds degradation.

The analysis of H_2O_2 production in synthetic urine revealed that the presence of organic compounds, such as urea, creatinine, and uric acid, in the synthetic urine matrix interfered with H_2O_2 accumulation, and this resulted in a decrease of 65% in H_2O_2 production compared to the concentration of H_2O_2 generated in the aqueous solution containing only Na_2SO_4 (at the current density of 50 mA cm^{-2}). This outcome was attributed to the consumption of H_2O_2 in the degradation of organic compounds. Additionally, it was demonstrated that the ionic composition of urine further limited H_2O_2 production, and this clearly reflects the complexity of the reactions involved. Energy efficiency analysis showed that the Na_2SO_4 solution exhibited lower energy consumption and higher current efficiency compared to the synthetic urine matrix - both in the presence and absence of organic compounds, which exhibited higher energy consumption and lower current efficiency. The results obtained from these analyses show that the presence of inorganic ions in synthetic urine significantly affected the H_2O_2 electro-generation efficiency. In particular, the presence of chloride and phosphate ions exerted a negative impact on H_2O_2 electro-generation, by either competing with reagents on the electrode surface or promoting secondary reactions that consumed the H_2O_2 generated.

Regarding the oxidation of organic matter in synthetic urine, the data obtained showed that the *in situ* generation of H_2O_2 in the matrix enhances the degradation of complex organic

compounds, with increased efficiency in the removal of urea (8.3%) and creatinine (8.6%). Kinetic analysis pointed to the preference of the system for the degradation of uric acid; in essence, the results of this analysis highlighted the importance of chemical interactions in the degradation process. The mineralization of the organic compounds, although limited to 31.8% TOC removal, showed that H_2O_2 may act as a complementary degradation agent in complex wastewater treatment systems. The high concentration of carboxylic acids, particularly oxalic and maleic acids, accumulated in the system was regarded as the primary intermediate products of the degradation process. Of the nitrogenous compounds formed in the oxidation process, we observed the initial release/formation of NH_4^+, which was subsequently oxidized to NO_3^-.

The findings of this study show that the *in situ* generation of H_2O_2 is a highly promising alternative technique for the treatment of urinary effluents; this technique is found to promote greater energy efficiency and partial mineralization of organic compounds. When it comes to the treatment of complex matrices, it becomes evident that, in addition to organic compounds, one needs to also consider the complex nature of inorganic compounds. Understanding the specific role of each inorganic ion present in urine is essential for developing more efficient treatment techniques that are capable of optimizing the electrochemical process, while reducing energy consumption and maximizing current efficiency. This study not only elucidates the mechanisms involved in H_2O_2 electro-generation in both organic and inorganic matrices but also provides significant contributions to the advancement of electro-sanitation technologies. Given the importance of these findings, future studies will focus on translating this knowledge to real urine matrices, further enhancing the sustainable treatment of decentralized wastewater systems and accelerating progress toward the accomplishment of SDG 6.

Acknowledgements

This study was financed, in part, by the São Paulo Research Foundation (FAPESP), Brazil. Process Number (#2023/13260-2, #2023/06558-5, #2020/02743-4, #2018/22210-0, #2018/22211-7, #2018/22022-0, #2019/06650-3 and #2022/12895-1) and the Brazilian National Council for Scientific and Technological Development – CNPq (grant #303943/2021-1).

Author contributions

All authors contributed to the study conception and design. **Raul José Alves Felisardo:** Conceptualization, methodology, investigation, validation, formal analysis, visualization, data curation, writing - original draft, writing - review &editing. **Carlos Henrique Magalhães Fernandes:** Investigation, validation, formal analysis, writing - original draft, writing - review & editing. **Géssica de Oliveira Santiago Santos:** Investigation, validation, formal analysis, writing - original draft, writing - review & editing. **Marcos Roberto de Vasconcelos Lanza**: Conceptualization, supervision, project administration, funding acquisition, writing - review & editing. All authors read and gave their approval of the final manuscript.

882

883 **References**

884 [1] W. Leal Filho, L. Viera Trevisan, I. Simon Rampasso, R. Anholon, M.A. Pimenta Dinis, L.
885 Londero Brandli, J. Sierra, A. Lange Salvia, R. Pretorius, M. Nicolau, J.H. Paulino Pires
886 Eustachio, J. Mazutti, When the alarm bells ring: Why the UN sustainable development goals
887 may not be achieved by 2030, J Clean Prod 407 (2023) 137108.
888 https://doi.org/10.1016/j.jclepro.2023.137108.

889 [2] F. Fuso Nerini, M. Mazzucato, J. Rockström, H. van Asselt, J.W. Hall, S. Matos, Å. Persson, B.
890 Sovacool, R. Vinuesa, J. Sachs, Extending the Sustainable Development Goals to 2050 — a
891 road map, Nature 630 (2024) 555–558. https://doi.org/10.1038/d41586-024-01754-6.

892 [3] UNESCO, Imminent risk of a global water crisis, warns the UN World Water Development
893 Report 2023, Https://Www.Unesco.Org/Reports/Wwdr/2023/En (2024).

894 [4] S. Sorooshian, The sustainable development goals of the United Nations: A comparative
895 midterm research review, J Clean Prod 453 (2024) 142272.
896 https://doi.org/10.1016/j.jclepro.2024.142272.

897 [5] C. Rose, A. Parker, B. Jefferson, E. Cartmell, The Characterization of Feces and Urine: A Review
898 of the Literature to Inform Advanced Treatment Technology, Crit Rev Environ Sci Technol 45
899 (2015) 1827–1879. https://doi.org/10.1080/10643389.2014.1000761.

900 [6] S. Dbira, N. Bensalah, M.I. Ahmad, A. Bedoui, Electrochemical Oxidation/Disinfection of Urine
901 Wastewaters with Different Anode Materials, Materials 12 (2019) 1254.
902 https://doi.org/10.3390/ma12081254.

903 [7] T.L. Chipako, D.G. Randall, Urine treatment technologies and the importance of pH, J Environ
904 Chem Eng 8 (2020) 103622. https://doi.org/10.1016/j.jece.2019.103622.

905 [8] S. Moharramzadeh, S.K. Ong, J. Alleman, K.S. Cetin, Stabilization and concentration of
906 nitrogen in synthetic urine with peracetic acid and progressive freeze concentration, J Environ
907 Chem Eng 10 (2022) 107768. https://doi.org/10.1016/j.jece.2022.107768.

908 [9] J. Senecal, B. Vinnerås, Urea stabilisation and concentration for urine-diverting dry toilets:
909 Urine dehydration in ash, Science of The Total Environment 586 (2017) 650–657.
910 https://doi.org/10.1016/j.scitotenv.2017.02.038.

911 [10] M. Ikematsu, K. Kaneda, M. Iseki, M. Yasuda, Electrochemical treatment of human urine for its
912 storage and reuse as flush water, Science of The Total Environment 382 (2007) 159–164.
913 https://doi.org/10.1016/j.scitotenv.2007.03.028.

914 [11] R.J.A. Felisardo, G.N. dos Santos, M.S. Leite, L.F.R. Ferreira, S. Garcia-Segura, E.B. Cavalcanti,
915 Decentralized electro-sanitation system as proof of concept to treat urine produced in long-
916 distance bus, Process Safety and Environmental Protection (2023).
917 https://doi.org/10.1016/j.psep.2023.11.065.

918 [12] A.J. dos Santos, H.L. Barazorda-Ccahuana, G. Caballero-Manrique, Y. Chérémond, P.J.
919 Espinoza-Montero, J.R. González-Rodríguez, U.J. Jáuregui-Haza, M.R. V. Lanza, A. Nájera, C.

Oporto, A. Pérez Parada, T. Pérez, V.D. Quezada, V. Rojas, V. Sosa, A. Thiam, R.A. Torres-Palma, R. Vargas, S. Garcia-Segura, Author Correction: Accelerating innovative water treatment in Latin America, Nat Sustain (2023). https://doi.org/10.1038/s41893-023-01075-y.

[13] T.A. Larsen, M.E. Riechmann, K.M. Udert, State of the art of urine treatment technologies: A critical review., Water Res X 13 (2021) 100114. https://doi.org/10.1016/j.wroa.2021.100114.

[14] Y. Yang, N.C. Ramos, J.A. Clark, H.W. Hillhouse, Electrochemical oxidation of pharmaceuticals in synthetic fresh human urine: Using selective radical quenchers to reveal the dominant degradation pathways and the scavenging effects of individual urine constituents, Water Res 221 (2022) 118722. https://doi.org/10.1016/j.watres.2022.118722.

[15] R.J.A. Felisardo, E. Brillas, T.H. Boyer, E.B. Cavalcanti, S. Garcia-Segura, Electrochemical degradation of acetaminophen in urine matrices: Unraveling complexity and implications for realistic treatment strategies, Water Res 261 (2024) 122034. https://doi.org/10.1016/j.watres.2024.122034.

[16] M.Y.D. Alazaiza, A. Albahnasawi, M. Eyvaz, D.E. Nassani, S.S. Abu Amr, M.S.S. Abujazar, O. Al-Maskari, Electrochemical-based advanced oxidation for hospital wastewater treatment, Desalination Water Treat 300 (2023) 44–56. https://doi.org/10.5004/dwt.2023.29714.

[17] C. Yang, Y. Fan, P. Li, Q. Gu, X. Li, Freestanding 3-dimensional macro-porous SnO2 electrodes for efficient electrochemical degradation of antibiotics in wastewater, Chemical Engineering Journal 422 (2021) 130032. https://doi.org/10.1016/j.cej.2021.130032.

[18] Q. Zhou, Z. Yan, Y. Lan, Z. Ou, R. Hu, X. Wang, Z. Yang, Y. Chen, J. Cai, Q. Lu, S. Wang, J.C. Yu, L. Li, Z. Hu, A general strategy to enhance hydrogen peroxide generation via two-electron water oxidation by antimony modification for removal of triethyl phosphate and hexavalent chromium, Appl Catal B 342 (2024) 123427. https://doi.org/10.1016/j.apcatb.2023.123427.

[19] Z. Yan, Y. Zhang, Z. Jiang, D. Jiang, W. Wei, Z. Hu, Nitrogen-Doped Bimetallic Carbide-Graphite Composite as Highly Active and Extremely Stable Electrocatalyst for Oxygen Reduction Reaction in Alkaline Media, Adv Funct Mater 32 (2022). https://doi.org/10.1002/adfm.202204031.

[20] W. Zhou, X. Meng, J. Gao, A.N. Alshawabkeh, Hydrogen peroxide generation from O2 electroreduction for environmental remediation: A state-of-the-art review, Chemosphere 225 (2019) 588–607. https://doi.org/10.1016/j.chemosphere.2019.03.042.

[21] R.B. Valim, J.F. Carneiro, J.C. Lourenço, P. Hammer, M.C. dos Santos, L.A. Rodrigues, R. Bertazzoli, M.R. de Vasconcelos Lanza, R. da Silva Rocha, Synthesis of Nb2O5/C for H2O2 electrogeneration and its application for the degradation of levofloxacin, J Appl Electrochem 54 (2024) 581–595. https://doi.org/10.1007/s10800-023-01975-z.

[22] J.F. Carneiro, R.S. Rocha, P. Hammer, R. Bertazzoli, M.R.V. Lanza, Hydrogen peroxide electrogeneration in gas diffusion electrode nanostructured with Ta2O5, Appl Catal A Gen 517 (2016) 161–167. https://doi.org/10.1016/j.apcata.2016.03.013.

[23] P.J. Marques Cordeiro-Junior, C. Sáez Jiménez, M.R. de Vasconcelos Lanza, M.A. Rodrigo Rodrigo, Electrochemical production of extremely high concentrations of hydrogen peroxide

in discontinuous processes, Sep Purif Technol 300 (2022) 121847. https://doi.org/10.1016/j.seppur.2022.121847.

[24] P.H. Arve, S.C. Popat, Stabilization of Urea for Recovery from Source-Separated Urine Using Electrochemically Synthesized Hydrogen Peroxide, ACS ES&T Engineering 1 (2021) 1642–1648. https://doi.org/10.1021/acsestengg.1c00194.

[25] G.N. Lewis, M. Randall, THE ACTIVITY COEFFICIENT OF STRONG ELECTROLYTES. [1], J Am Chem Soc 43 (1921) 1112–1154. https://doi.org/10.1021/ja01438a014.

[26] T. O. Silva, L. A. Goulart, I. Sánchez-Montes, G. O. S. Santos, R. B. Santos, R. Colombo, M. R. V. Lanza, Using a novel gas diffusion electrode based on PL6 carbon modified with benzophenone for efficient H2O2 electrogeneration and degradation of ciprofloxacin, Chemical Engineering Journal 455 (2023) 140697. https://doi.org/10.1016/j.cej.2022.140697.

[27] P.J.M. Cordeiro-Junior, J. Lobato Bajo, M.R. de V. Lanza, M.A. Rodrigo Rodrigo, Highly Efficient Electrochemical Production of Hydrogen Peroxide Using the GDE Technology, Ind Eng Chem Res 61 (2022) 10660–10669. https://doi.org/10.1021/acs.iecr.2c01669.

[28] X.-S. Chai, Q.X. Hou, Q. Luo, J.Y. Zhu, Rapid determination of hydrogen peroxide in the wood pulp bleaching streams by a dual-wavelength spectroscopic method, Anal Chim Acta 507 (2004) 281–284. https://doi.org/10.1016/j.aca.2003.11.036.

[29] G.W. Watt, J.D. Chrisp, Spectrophotometric Method for Determination of Urea, Anal Chem 26 (1954) 452–453. https://doi.org/10.1021/ac60087a006.

[30] F.-Y. Chen, Z.-Y. Wu, S. Gupta, D.J. Rivera, S. V. Lambeets, S. Pecaut, J.Y.T. Kim, P. Zhu, Y.Z. Finfrock, D.M. Meira, G. King, G. Gao, W. Xu, D.A. Cullen, H. Zhou, Y. Han, D.E. Perea, C.L. Muhich, H. Wang, Efficient conversion of low-concentration nitrate sources into ammonia on a Ru-dispersed Cu nanowire electrocatalyst, Nat Nanotechnol 17 (2022) 759–767. https://doi.org/10.1038/s41565-022-01121-4.

[31] M. Dan, R. Zhong, S. Hu, H. Wu, Y. Zhou, Z.-Q. Liu, Strategies and challenges on selective electrochemical hydrogen peroxide production: Catalyst and reaction medium design, Chem Catalysis 2 (2022) 1919–1960. https://doi.org/10.1016/j.checat.2022.06.002.

[32] G. Coria, T. Pérez, I. Sirés, J.L. Nava, Mass transport studies during dissolved oxygen reduction to hydrogen peroxide in a filter-press electrolyzer using graphite felt, reticulated vitreous carbon and boron-doped diamond as cathodes, Journal of Electroanalytical Chemistry 757 (2015) 225–229. https://doi.org/10.1016/j.jelechem.2015.09.031.

[33] Y. Duan, D.L. Sedlak, Electrochemical Hydrogen Peroxide Generation and Activation Using a Dual-Cathode Flow-Through Treatment System: Enhanced Selectivity for Contaminant Removal by Electrostatic Repulsion, Environ Sci Technol 58 (2024) 14042–14051. https://doi.org/10.1021/acs.est.4c05481.

[34] J. Moreira, V. Bocalon Lima, L. Athie Goulart, M.R.V. Lanza, Electrosynthesis of hydrogen peroxide using modified gas diffusion electrodes (MGDE) for environmental applications: Quinones and azo compounds employed as redox modifiers, Appl Catal B 248 (2019) 95–107. https://doi.org/10.1016/j.apcatb.2019.01.071.

[35] G. Grabner, N. Getoff, F. Schwörer, Pulsradiolyse von H3PO4, H2PO4-, HPO42− und P2O74− in wässriger lösung—II. Spektren und kinetik der Zwischenprodukte, International Journal for Radiation Physics and Chemistry 5 (1973) 405–417. https://doi.org/10.1016/0020-7055(73)90003-X.

[36] W. Yan, L. Wang, C. Jing, Phosphate ligand-mediated production of reactive oxygen species during oxygenation of Fe(II)-phosphate complexes, J Hazard Mater 479 (2024) 135720. https://doi.org/10.1016/j.jhazmat.2024.135720.

[37] M.S. Kronka, G. V. Fortunato, L. Mira, A.J. dos Santos, M.R.V. Lanza, Using Au NPs anchored on ZrO2/carbon black toward more efficient H2O2 electrogeneration in flow-by reactor for carbaryl removal in real wastewater, Chemical Engineering Journal 452 (2023) 139598. https://doi.org/10.1016/j.cej.2022.139598.

[38] J.R. Steter, E. Brillas, I. Sirés, On the selection of the anode material for the electrochemical removal of methylparaben from different aqueous media, Electrochim Acta 222 (2016) 1464–1474. https://doi.org/10.1016/j.electacta.2016.11.125.

[39] A.J. dos Santos, A.S. Fajardo, M.S. Kronka, S. Garcia-Segura, M.R.V. Lanza, Effect of electrochemically-driven technologies on the treatment of endocrine disruptors in synthetic and real urban wastewater, Electrochim Acta 376 (2021) 138034. https://doi.org/10.1016/j.electacta.2021.138034.

[40] J.M. Hermida-Ramón, A. Öhrn, G. Karlström, Planar or Nonplanar: What Is the Structure of Urea in Aqueous Solution?, J Phys Chem B 111 (2007) 11511–11515. https://doi.org/10.1021/jp073579x.

[41] Y. Zhang, Z. Li, Y. Zhao, S. Chen, I.B. Mahmood, Stabilization of source-separated human urine by chemical oxidation, Water Science and Technology 67 (2013) 1901–1907. https://doi.org/10.2166/wst.2013.055.

[42] D.G. Randall, V. Naidoo, Urine: The liquid gold of wastewater, J Environ Chem Eng 6 (2018) 2627–2635. https://doi.org/10.1016/j.jece.2018.04.012.

[43] K.M. Udert, T.A. Larsen, M. Biebow, W. Gujer, Urea hydrolysis and precipitation dynamics in a urine-collecting system, Water Res 37 (2003) 2571–2582. https://doi.org/10.1016/S0043-1354(03)00065-4.

[44] A. Patel, A.A. Mungray, A.K. Mungray, Technologies for the recovery of nutrients, water and energy from human urine: A review, Chemosphere 259 (2020) 127372. https://doi.org/10.1016/j.chemosphere.2020.127372.

[45] M. Cataldo Hernández, N. Russo, M. Panizza, P. Spinelli, D. Fino, Electrochemical oxidation of urea in aqueous solutions using a boron-doped thin-film diamond electrode, Diam Relat Mater 44 (2014) 109–116. https://doi.org/10.1016/j.diamond.2014.02.006.

[46] L.A. Goulart, A. Moratalla, P. Cañizares, M.R.V. Lanza, C. Sáez, M.A. Rodrigo, High levofloxacin removal in the treatment of synthetic human urine using Ti/MMO/ZnO photo-electrocatalyst, J Environ Chem Eng 10 (2022) 107317. https://doi.org/10.1016/j.jece.2022.107317.

[47] R.J.A. Felisardo, E. Brillas, L.F. Romanholo Ferreira, E.B. Cavalcanti, S. Garcia-Segura, Degradation of the antibiotic ciprofloxacin in urine by electrochemical oxidation with a DSA anode, Chemosphere 344 (2023) 140407. https://doi.org/10.1016/j.chemosphere.2023.140407.

[48] R.J.A. Felisardo, E. Brillas, E. Bezerra Cavalcanti, S. Garcia-Segura, Revealing degradation of organic constituents of urine during the electrochemical oxidation of ciprofloxacin via boron-doped diamond anode, Sep Purif Technol 331 (2024) 125655. https://doi.org/10.1016/j.seppur.2023.125655.

[49] I.M.D. Gonzaga, A. Moratalla, K.I.B. Eguiluz, G.R. Salazar-Banda, P. Cañizares, M.A. Rodrigo, C. Saez, Novel Ti/RuO2IrO2 anode to reduce the dangerousness of antibiotic polluted urines by Fenton-based processes, Chemosphere 270 (2021) 129344. https://doi.org/10.1016/j.chemosphere.2020.129344.

[50] M. Brienza, S. Garcia-Segura, Electrochemical oxidation of fipronil pesticide is effective under environmental relevant concentrations, Chemosphere 307 (2022) 135974. https://doi.org/10.1016/j.chemosphere.2022.135974.

[51] R.J.A. Felisardo, E. Brillas, T.H. Boyer, E.B. Cavalcanti, S. Garcia-Segura, Understanding electrochemical treatment of real fresh and hydrolyzed urine matrices to remove trace pharmaceuticals, Sep Purif Technol 342 (2024) 127016. https://doi.org/10.1016/j.seppur.2024.127016.

[52] M. Herraiz-Carboné, S. Cotillas, E. Lacasa, Á. Moratalla, P. Cañizares, M.A. Rodrigo, C. Sáez, Improving the biodegradability of hospital urines polluted with chloramphenicol by the application of electrochemical oxidation, Science of The Total Environment 725 (2020) 138430. https://doi.org/10.1016/j.scitotenv.2020.138430.

[53] A.M. Polcaro, A. Vacca, M. Mascia, F. Ferrara, Product and by-product formation in electrolysis of dilute chloride solutions, J Appl Electrochem 38 (2008) 979–984. https://doi.org/10.1007/s10800-008-9509-3.

[54] G.O.S. Santos, K.I.B. Eguiluz, G.R. Salazar-Banda, C. Sáez, M.A. Rodrigo, Understanding the electrolytic generation of sulfate and chlorine oxidative species with different boron-doped diamond anodes, Journal of Electroanalytical Chemistry 857 (2020) 113756. https://doi.org/10.1016/j.jelechem.2019.113756.

[55] G.O.S. Santos, K.I.B. Eguiluz, G.R. Salazar-Banda, C. Saez, M.A. Rodrigo, Photoelectrolysis of clopyralid wastes with a novel laser-prepared MMO-RuO2TiO2 anode, Chemosphere 244 (2020) 125455. https://doi.org/10.1016/j.chemosphere.2019.125455.

[56] E.B. Cavalcanti, S.G. -Segura, F. Centellas, E. Brillas, Electrochemical incineration of omeprazole in neutral aqueous medium using a platinum or boron-doped diamond anode: Degradation kinetics and oxidation products, Water Res 47 (2013) 1803–1815. https://doi.org/10.1016/j.watres.2013.01.002.

[57] V.S. Antonin, M.C. Santos, S. Garcia-Segura, E. Brillas, Electrochemical incineration of the antibiotic ciprofloxacin in sulfate medium and synthetic urine matrix, Water Res 83 (2015) 31–41. https://doi.org/10.1016/j.watres.2015.05.066.

[58] A.J. dos Santos, G. V. Fortunato, M.S. Kronka, L.G. Vernasqui, N.G. Ferreira, M.R.V. Lanza, Electrochemical oxidation of ciprofloxacin in different aqueous matrices using synthesized boron-doped micro and nano-diamond anodes, Environ Res 204 (2022) 112027. https://doi.org/10.1016/j.envres.2021.112027.

Highlights

- Inorganic urine composition significantly influences *in situ* H_2O_2 generation
- Active chlorine species affect the accumulation of H_2O_2 in urine
- *In situ* H_2O_2 generation enhances the removal of organic compounds in urine
- Uric acid is degraded 95 times faster than urea and 15 times faster than creatinine
- *In situ* H_2O_2 generation contributes to sustainable treatment of sanitary effluents.